PHYSICAL REVIEW C **72**, 041302(R) (2005)

Lifetime of the astrophysically important 4.03-MeV state in ^{19}Ne

W. P. Tan, J. Görres, J. Daly, M. Couder, A. Couture, H. Y. Lee, E. Stech, E. Strandberg, C. Ugalde, and M. Wiescher
Department of Physics, University of Notre Dame, Notre Dame, Indiana 46556, USA

(Received 20 June 2005; published 28 October 2005)

The ^{15}O$(\alpha,\gamma)^{19}$Ne reaction is one of the most important breakout reactions for the hot CNO cycles. However, the relevant states in ^{19}Ne at excitation energies of 4–5 MeV have not been well studied. The lifetimes of these states are not known and are only constrained by experimental upper and lower limits. In particular, accurate knowledge of the γ- and α-decay widths of the 4.03-MeV state of ^{19}Ne is important, since the resonance strength of this level dominates the reaction rate for the astrophysically relevant temperatures $T_9 < 0.6$. In this work, we employed an improved Doppler-shifted attenuation method to obtain lifetime values of this and other states via ^{17}O(^{3}He, n-γ)^{19}Ne. For the 4.03-MeV state, the measured excitation energy is 4034.5 ± 0.8 keV and the mean lifetime, measured here for the first time, is 13^{+9}_{-6} fs at the confidence level of 1σ and 13^{+16}_{-9} fs at the confidence level of 2σ. This result is in excellent agreement with the 9-fs prediction by Langanke, Wiescher, Fowler, and Görres.

DOI: 10.1103/PhysRevC.72.041302 PACS number(s): 27.20.+n, 21.10.Tg, 25.55.Hp, 26.50.+x

The hot CNO cycles and the ensuing *rp*-process after breakout play a principal role in the energy production and nucleosynthesis of explosive hydrogen-burning processes occurring in astrophysical sites such as novae and accreting neutron stars [1–4]. The reaction ^{15}O$(\alpha,\gamma)^{19}$Ne provides the initial breakout route from the hot CNO cycles, triggering the *rp*-process [1]. The strength of this reaction determines the abundance of ^{15}N in novae ejecta and the possible feeding of the NeNa cycle in high-temperature nova explosions [5]. A more dramatic impact however is anticipated for thermonuclear runaway in accreting neutron stars, which are observed as x-ray bursts. Calculations have shown that the luminosity of x-ray bursters is dramatically increased by the breakout from the hot CNO cycles owing to the subsequent energy produced by the *rp*-process [1]. Multimass zone model simulations of the evolution of x-ray bursters indicate that the ^{15}O$(\alpha,\gamma)^{19}$Ne reaction rate actually provides the trigger conditions for periodic x-ray bursters [6]. Both theoretical and experimental aspects of this breakout reaction have been studied over the past years [7–15]. The direct capture contribution is negligible at temperatures $T_9 > 0.1$ [7] and the reaction rate can be expressed as a sum of all resonance contributions [16],

$$N_A\langle\sigma v\rangle_{\rm res} \propto (kT)^{-3/2}\sum\frac{\Gamma^i_\alpha\Gamma^i_\gamma}{\Gamma^i_\alpha+\Gamma^i_\gamma}\frac{(J_i+1)}{2}\exp(-E_i/kT), \tag{1}$$

where J_i, E_i, Γ^i_α, and Γ^i_γ represent the spin, energy, and α- and γ-decay widths of resonance i.

The partial widths Γ_α and Γ_γ of the relevant states with excitation energies of 4–5 MeV are not sufficiently well known for reliably calculating the reaction rate. All previous attempts have, therefore, relied on information taken from the analog states in ^{19}F. Of particular interest is the resonance at an excitation energy of 4.03 MeV in ^{19}Ne, just above the ^{15}O+α threshold. This resonance dominates the reaction rate at temperatures below 0.6 GK [7] and determines therefore the temperature conditions for the breakout from the hot CNO cycles. A direct measurement of the resonance strength is not feasible with the presently available intensities of radioactive ^{15}O beams. The main focus is therefore the measurement of the relative α partial width $\Gamma_\alpha/\Gamma_{\rm tot}$. By using these values in conjunction with the lifetimes of the states the resonance strengths can be directly calculated. The relative α widths of the resonance states in ^{19}Ne have been successfully measured [8] except for the critical level at 4.03 MeV. The main obstacle is the extremely small branching ratio $\Gamma_\alpha/\Gamma_\gamma$, which has been predicted to be of the order of 10^{-4} [7]. Its measurement has been attempted by various groups [10–14] but only upper limits could be established in these studies.

The critical parameters for deriving the resonance strengths from the relative α widths are the total widths or lifetimes of the resonance states. This information is not known for any of the resonance states in question. Previous attempts to determine the lifetimes have provided only upper limits for the lifetimes of the unbound states near the α threshold (see the TUNL compilation of Ref. [17]) with the Doppler-shift attenuation method (DSAM) [18]. A recent approach of a direct measurement of the lifetimes made using the the Coulomb excitation technique resulted only in an lower limit of 1.5 fs for the lifetime of the 4.03-MeV level [19]. In this work, we successfully employed an improved DSAM approach to obtain lifetime values for this state and other threshold states via ^{17}O(^{3}He, n-γ)^{19}Ne.

The experiment was conducted using the KN Van de Graaff accelerator at the University of Notre Dame. A 3.0-MeV ^{3}He beam with average intensity of 12 μA was directed upon an implanted ^{17}O target with Ta backing. The target was prepared by implanting a low dose of ^{17}O ions (1.25×10^{17}/cm^2) with an implantation energy of 70 keV. An ORTEC HPGe detector with an active volume of 225 cm^3 was used to measure γ rays from ^{19}Ne decay in coincidence with neutrons detected with a liquid scintillation detector. Three geometries were used to obtain the Doppler-shifted γ spectra. The unshifted γ energy is obtained by averaging two γ spectra measured by the same Ge detector at 45° and 135°, respectively, in coincidence with neutrons detected at 0° with respect to the beam direction. An

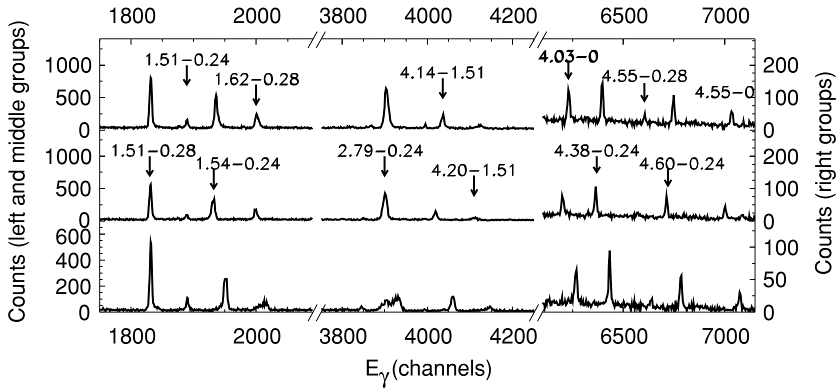

FIG. 1. γ spectra, from top to bottom, respectively, for the 45°, 135°, and 0° setups. Three groups of peaks from the significant transitions of the states in ^{19}Ne are shown in each panel. See text for detailed discussion.

advantage of using the symmetrically Doppler-shifted spectra is that geometric uncertainties of the detector setup cancel out. In the third geometry, γ rays were measured at 28.5° and neutrons at 90° to maximize the Doppler shift as the angle between emitting γ ray and recoiling ^{19}Ne is 0° (denoted as 0° setup in the rest of the paper).

Well-known γ energies from the in-beam reactions of ^{17}O(^{3}He,d-γ), ^{17}O(^{3}He,p-γ), and ^{12}C(^{3}He,p-γ) were recorded simultaneously with the γ transitions from ^{19}Ne and used for the energy calibration of the Ge detector. In addition, the energy resolution of the Ge detector was measured as a function of energy and used for the simulation analysis with GEANT4.

In Fig. 1, the raw γ spectra in coincidence with neutrons are shown for the portions relevant to the states in ^{19}Ne. Spectra shown in the top and middle panels were measured in the 45° and 135° setups, respectively, for the determination of unshifted γ energies. The spectrum shown in the bottom panel has been obtained with the maximized Doppler-shift (0°) setup. In this setup, the peaks are not only significantly shifted but broadened as well. Particularly, the transition from 2.79 to 0.24 states shows a double-peak structure, which corresponds to contributions from both stopped and moving ^{19}Ne in the target. In less extreme cases such as the transition 1.62 → 0.28, the broadened peak shows a significant low-energy tailing down to about the unshifted γ energy. The simple DSAM approach [18,20–22] widely used in the lifetime measurements takes into account only the Doppler shift of peak centroids and, therefore, is insufficient to study these cases. In this work, the improved DSAM is applied with full line-shape analysis using GEANT4 [23] simulation, which will be discussed later.

In Fig. 2, the γ spectra of the transition from the 4.03-MeV state to the ground state are plotted for the three experimental geometries. The spectra from the 45° and 135° setups are fitted and averaged to determine the unshifted γ energy and the corresponding excitation energy after correction for the γ recoil. This procedure yields an excitation energy of 4034.5 ± 0.8 keV for the 4.03-MeV $3/2^+$ state, which is slightly higher than (albeit in statistical agreement with) the currently accepted value [17].

The simulations of the γ-line Doppler broadening have been done with GEANT4 [23] for the 0° spectrum by adopting the unshifted γ energy obtained in this experiment and taking into account the calibrated energy response of the Ge detector and the geometry of the setup. The low-energy extensions to the GEANT4 electromagnetic processes are applied [24] and the stopping power model for the energy loss calculation has been adopted from the Ziegler parametrization [25–27]. Details of the analysis will be presented in a forthcoming publication [28] and the relevant aspects are summarized in the following. The sensitivity of the target profile and composition has been studied and has been found to be negligible. Because of the low implantation dose the stopping powers are dominated by the interaction with the Ta atoms [28,29]. Dependence on the stopping powers is also found to be insignificant [22,28]. Corrections for beam spread and beam direction, although insignificant, have been applied according to the bombarding spot on the target after the experiment. The data from the 0° setup have been fitted with GEANT4 simulations for various lifetime values, as shown in Fig. 3.

The solid line in Fig. 3 shows the best fit obtained for a lifetime of $\tau_m = 13$ fs. Fits for other lifetimes are also shown for comparison. The error of the lifetime is estimated by examining the χ^2 values of the fit as the lifetime is varied. At the 1σ confidence level the lifetime is 13^{+9}_{-6} fs and at the 2σ confidence level the value is 13^{+16}_{-9} fs. The dashed and dotted lines in Fig. 3 depict the 2σ limits with lifetimes of 4 and 29 fs,

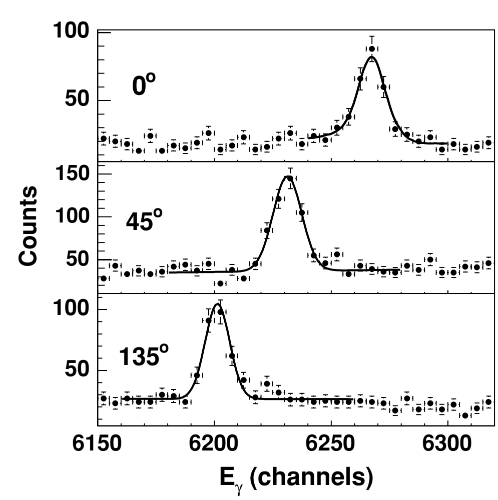

FIG. 2. γ spectra for the 4.03 → 0 transition plotted for the 0°, 45°, and 135° setups, respectively. The solid lines in the two lower panels are the fits for energy measurement. The solid line in the top panel is the best fit with the GEANT4 simulation at $\tau_m = 13$ fs (and is enlarged with more detail in Fig. 3).

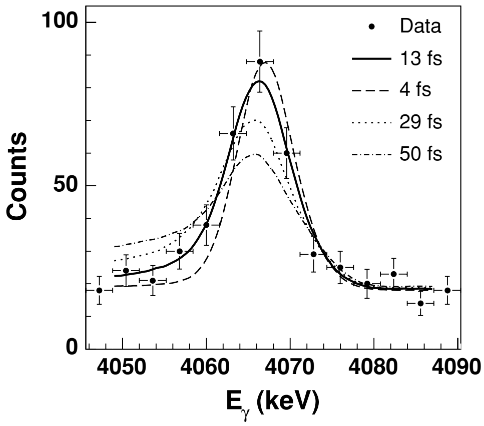

FIG. 3. Black dots are the experimental data of the γ transition $4.03 \rightarrow 0$ for the 0° setup. The solid line is the best fit with the GEANT4 simulation at $\tau_m = 13$ fs. The dashed and dotted lines depict lifetimes of 4 fs and 29 fs, respectively, representing the 2σ uncertainty limits of the analysis presented here. The dot-dashed line simulates the peak shape for a 50-fs lifetime, corresponding to the upper limit from previous measurements [18] and very close to the suggested value in Ref. [19]. See text for detailed discussion.

respectively. The smaller lifetime produces a narrower peak, which is also shifted to the high-energy side, whereas the larger lifetime results in peak broadening with a more noticeable low-energy tail. The dot-dashed line represents the previous upper limit of 50 fs set by Ref. [18], which is too broad and unable to account for both the peak height and the low-energy tail. The fit to the high-energy tailing or shoulder of the data is not sensitive to the input lifetime since it does not originate from the Doppler-shifted spectrum of $4.03 \rightarrow 0$ but results from the small contribution from the nearby single escape peak of the transition $4.55 \rightarrow 0$, which happens to hide the otherwise more pronounced asymmetry of the $4.03 \rightarrow 0$ line shape resulting from the Doppler effects. This was also taken into account in the simulation and has only an insignificant effect on the final result for the lifetime. In Ref. [19], a γ-decay width of 12^{+9}_{-5} meV was suggested (very close to the previous upper limit of 50-fs lifetime as shown in Fig. 3). This value had been deduced from the 1.5-fs lower limit for the lifetime set by the Coulomb excitation measurements and a theoretical calculation of the $E2/M1$ ratio. This value is more than a factor of 4 smaller than the one resulting from our new measurement.

Similar procedures have been carried out for other relevant states at excitation energies of 4–5 MeV. The resulting values for excitation energies and lifetimes are listed in Table I. The errors of the lifetime values are evaluated at the confidence level of 1σ in the χ^2 analysis. For comparison the currently adopted values from Ref. [17] are listed in the left column. The observed lifetimes of the ^{19}Ne bound states at 1.51, 1.54, 1.62, and 2.79 MeV are in statistical agreement with previous results but have significantly improved accuracy. The seemingly systematic discrepancy for the 1.54-, 1.62-, and 2.79-MeV states may lie in the simplified treatment in the previous measurements because the compilation data [17] of these states were based on the same technique and reaction used by those experiments [20–22].

In summary, an improved DSAM approach with a GEANT4 simulation has been applied to the γ-spectra data from the

TABLE I. Values of excitation energies and lifetimes of the states in ^{19}Ne from the present work with uncertainties on the lifetimes given at the 1σ confidence level. For reference, the adopted values from Ref. [17] are shown in the left column.

Compilation [17]			Present work	
E_X (keV)	J^π	τ_m (fs)	E_X (keV)	τ_m (fs)
1507.56 ± 0.3	$\frac{5}{2}-$	$1.4^{+0.5}_{-0.6} \times 10^3$	1507.51 ± 0.35	$1.7 \pm 0.3 \times 10^3$
1536.0 ± 0.4	$\frac{3}{2}+$	28 ± 11	1536.05 ± 0.36	16 ± 4
		(28 ± 15) [20]		
		(28^{+18}_{-16}) [21]		
1615.6 ± 0.5	$\frac{3}{2}-$	143 ± 31	1615.4 ± 0.4	80 ± 15
		(130 ± 35) [22]		
		(180 ± 60) [20]		
2794.7 ± 0.6	$\frac{9}{2}+$	140 ± 35	2794.2 ± 0.4	100 ± 12
		(140 ± 35) [22]		
		(330 ± 130) [20]		
4032.9 ± 2.4	$\frac{3}{2}+$	<50	4034.5 ± 0.8	13^{+9}_{-6}
4140 ± 4	$(\frac{9}{2})^-$	<300	4143.5 ± 0.6	18^{+2}_{-3}
4197.1 ± 2.4	$(\frac{7}{2})^-$	<350	4200.3 ± 1.1	43^{+12}_{-9}
4379.1 ± 2.2	$\frac{7}{2}+$	<120	4377.8 ± 0.6	5^{+3}_{-2}
4549 ± 4	$(\frac{1}{2}, \frac{3}{2})^-$	<80	4547.7 ± 1.0	15^{+11}_{-5}
4600 ± 4	$(\frac{5}{2}+)$	<160	4601.8 ± 0.8	7^{+5}_{-4}
4635 ± 4	$\frac{13}{2}+$	$>1 \times 10^3$	4634.0 ± 0.9	$>1 \times 10^3$

reaction ^{17}O(^{3}He, n-γ)^{19}Ne. The excitation energy values of all threshold states are improved and lifetimes for all states up to 4.6 MeV have been extracted. The lifetime of the important 4.03-MeV state has been determined for the first time to $\tau = 13^{+9}_{-6}$ fs at the confidence level of 1σ and 13^{+16}_{-9} fs at the confidence level of 2σ.

The present results represent significant improvements in the accuracy of the excitation energies and in the final experimental determination of the lifetimes. Both results reduce significantly the uncertainties in the reaction rate of ^{15}O(α, γ)^{19}Ne. The rates depend exponentially on the resonance energies but depend linearly on the product of the relative α widths $\Gamma_\alpha/\Gamma_{\rm tot}$ and the γ widths Γ_γ. Recent estimates of the reaction rate are based on a variety of estimates for these γ widths, which were either taken directly from lifetime measurements of ^{19}F mirror states [17] or were based on upper and lower limit arguments or shell model calculations [6,7,12–14]. These selected best values for γ widths, in particular for the two critical resonance states at 4.03 and 4.38 MeV, differ substantially from our work and among themselves by a factor of 3. Our new results remove these uncertainties, particularly reduce the uncertainty of the γ width of the 4.03-MeV state by a factor of 3, and will significantly improve our knowledge of the reaction rate of ^{15}O(α, γ)^{19}Ne.

This work is supported by the National Science Foundation under Grant No. PHY01-40324 and the Joint Institute for Nuclear Astrophysics, NSF-PFC, under Grant No. PHY02-16783.

[1] M. Wiescher, J. Görres, and H. Schatz, J. Phys. G **25**, 133(R) (1999).
[2] R. Wallace and S. Woosley, Astrophys. J. Suppl. **45**, 389 (1981).
[3] A. Champagne and M. Wiescher, Annu. Rev. Nucl. Part. Sci. **42**, 39 (1992).
[4] H. Schatz, A. Aprahamian, J. Görres, M. Wiescher, T. Rauscher, J. Rembges, F.-K. Thielemann, B. Pfeiffer, P. Möller, K.-L. Kratz *et al.*, Phys. Rep. **294**, 167 (1998).
[5] C. Iliadis, A. E. Champagne, J. Jose, S. Starrfield, and P. Tupper, Astrophys. J. Suppl. **142**, 105 (2002).
[6] J. L. Fisker, J. Görres, M. Wiescher, and B. Davids, submitted to Astrophys. J. arXiv:astro-ph/0410561.
[7] K. Langanke, M. Wiescher, W. Fowler, and J. Görres, Astrophys. J. **301**, 629 (1986).
[8] P. V. Magnus, M. S. Smith, A. J. Howard, P. D. Parker, and A. E. Champagne, Nucl. Phys. **A506**, 332 (1990).
[9] Z. Q. Mao, H. T. Fortune, and A. G. Lacaze, Phys. Rev. Lett. **74**, 3760 (1995).
[10] M. Kurokawa, K. I. Hahn, P. Strasser, S. Kubono, T. Koike, X. Liu, T. Miyachi, Y. Fuchi, S. C. Jeong, H. Kawashima *et al.*, in *International Symposium on Origin of Matter and Evolution of Galaxies 97: Atami, Japan, 5–7 November 1997*, edited by S. Kubono, T. Kajino, K. I. Nomoto, and I. Tanihata (World Scientific, Singapore, New Jersey, 1998), p. 245.
[11] A. M. Laird, S. Cherubini, A. N. Ostrowski, M. Aliotta, T. Davinson, A. D. Pietro, P. Figuera, W. Galster, J. S. Graulich, D. Groombridge *et al.*, Phys. Rev. C **66**, 048801 (2002).
[12] K. E. Rehm, A. H. Wuosmaa, C. L. Jiang, J. Caggiano, J. P. Greene, A. Heinz, D. Henderson, R. V. F. Janssens, E. F. Moore, G. Mukherjee *et al.*, Phys. Rev. C **67**, 065809 (2003).
[13] B. Davids, A. van den Berg, P. Dendooven, F. Fleurot, M. Hunyadi, M. de Huu, K. Rehm, R. Segel, R. Siemssen, H. Wilschut *et al.*, Phys. Rev. C **67**, 012801(R) (2003).
[14] B. Davids, A. M. van den Berg, P. Dendooven, F. Fleurot, M. Hunyadi, M. A. de Huu, R. H. Siemssen, H. W. Wilschut, H. J. Wörtche, M. Hernanz *et al.*, Phys. Rev. C **67**, 065808 (2003).
[15] D. W. Visser, J. A. Caggiano, R. Lewis, W. B. Handler, A. Parikh, and P. D. Parker, Phys. Rev. C **69**, 048801 (2004).
[16] C. E. Rolfs and W. S. Rodney, *Cauldrons in the Cosmos* (University of Chicago, Chicago, 1988).
[17] D. Tilley, H. Weller, C. Cheves, and R. Chasteler, Nucl. Phys. **A595**, 1 (1995).
[18] J. Davidson and M. Roush, Nucl. Phys. **A213**, 332 (1973).
[19] G. Hackman, S. M. Austin, T. Glasmacher, T. Aumann, B. A. Brown, R. W. Ibbotson, K. Miller, B. Pritychenko, L. A. Riley, B. Roeder *et al.*, Phys. Rev. C **61**, 052801(R) (2000).
[20] R. D. Gill, K. Bharuth-Ram, K. P. Jackson, R. A. I. Bell, B. C. Robertson, J. L'Ecuyer, N. G. Chapman, and H. J. Rose, Nucl. Phys. **A152**, 369 (1970).
[21] T. Itahashi, T. Shibata, and T. Wakatsuki, J. Phys. Soc. Jpn. **31**, 961 (1971).
[22] C. Lebrun, F. Guilbault, P. Avignon, and Y. Deschamps, Phys. Rev. C **15**, 1174 (1977).
[23] S. Agostinelli, J. Allison, K. Amako, J. Apostolakis, H. Araujo, P. Arce, M. Asai, D. Axen, S. Banerjee, G. Barrand *et al.* (GEANT4 Collaboration), Nucl. Instrum. Methods Phys. Res. A **506**, 250 (2003).
[24] S. Chauvie, G. Depaola, V. Ivanchenko, F. Longo, P. Nieminen, and M. Pia, in *Proceedings of Computing in High Energy Physics* (Beijing, 2001), http://www.ge.infn.it/geant4/lowE/index.html.
[25] H. Andersen and J. Ziegler, *The Stopping and Ranges of Ions in Matter*, Vol. 3 (Pergamon, London, 1977).
[26] J. F. Ziegler, J. P. Biersack, and U. Littmark, *The Stopping and Ranges of Ions in Solids*, Vol. 1 (Pergamon, London, 1985).
[27] Srim-2003, http://www.srim.org.
[28] W. P. Tan *et al.*, in preparation.
[29] S. Seuthe, H. W. Becker, A. Krauss, A. Redder, C. Rolfs, U. Schröder, H. P. Trautvetter, K. Wolke, S. Wüstenbecker, R. W. Kavanagh *et al.*, Nucl. Instrum. Methods Phys. Res. A **260**, 33 (1987).